Research Article | Vol. 26, No. 25 | 10 Dec 2018 | OPTICS EXPRESS 32417
Optics EXPRESS

Micro-fluorescence lifetime and spectral imaging of ytterbium doped laser materials

T. SCHREIBER,[1,*] S. KUHN,[1] G. FELDKAMP,[1] A. SCHWUCHOW,[2] K. SCHUSTER,[2] S. HEIN,[1] R. EBERHARDT,[1] AND A. TÜNNERMANN[1]

[1]*Fraunhofer Institute for Applied Optics and Precision Engineering IOF, Albert-Einstein-Strasse 7, 07745 Jena, Germany*
[2]*Leibniz Institute of Photonic Technology, Albert-Einstein-Strasse 9, 07745 Jena, Germany*
**thomas.schreiber@iof.fraunhofer.de*

Abstract: We present the application of a confocal fluorescence microscope to the analysis of Yb-doped solid-state laser materials, with examples of Yb-doped crystals, photonic crystal fibers and fiber preforms made with different manufacturing processes. Beside the fluorescence lifetime image itself, a microscopic spectral fluorescence emission analysis is presented and spatially resolved emission cross sections are obtained. Doping concentration and its distributions and other laser optical parameters are measured, which help to analyze manufacturing steps. Further properties like photodarkening and saturation are addressed.

1. Introduction

It is unquestionable that rare-earth doped materials contributed significantly to the development of solid-state and fiber lasers [1,2]. The properties of the doped material have a huge influence on the performance of the final laser configuration. This is especially true for fiber lasers, where both the refractive index profile and the laser parameters of the dopants play a crucial role [3]. Additionally, long-term operation of such lasers can be optimized by reducing photodarkening (PD) of the doped materials and limiting thermos-optical effects, like transverse mode instabilities [4], might be reduced. In order to evaluate and influence the materials properties during the design and fabrication steps, its monitoring and quantitative measurement is of greatest importance.

Measuring the refractive index distribution but especially the of rare-earth ion's distribution in the fiber or preform is one task for quality monitoring. In simply terms, this is useful for guaranteeing the core's desired design by predicting the guiding properties and fix the drawing geometries. Due to various processing steps, especially under high temperatures, the refractive index distribution as well as the dopant distribution might change, for instance, due to diffusion, crystallization or mechanical stress.

For monitoring the local dopant distribution, many possibilities are known with special limitations in spatial and concentration resolution, effort of preparation and cost. A very good overview is given in [5] with the analysis and comparison of material science methods and optical analysis techniques. Due to its simplicity and component availability optical methods appear to be interesting for characterization and have been done mostly for Er-doped fibers. There is another advantage for optical methods: If the observation is linked to the actual properties of the rare-earth ion, specific laser parameters can be determined. For fluorescence analysis, this includes at least upper state fluorescence lifetime and intensity, from which the local dopant distribution is obtained, as well as the emission spectrum. Different methods are known with certain advantages, like the twice-perpendicular measurements [6], spatial resolved but non-destructive interferometric methods [7] or microscopes. For the latter method, a typical confocal fluorescence microscope is readily available in most labs and only needs to be adapted to the desired wavelength [8]. Fluorescence lifetime imaging is well established in biomedical environments [9]. However, for the case of many lanthanides used

#344533 https://doi.org/10.1364/OE.26.032417
Journal © 2018 Received 3 Sep 2018; revised 19 Oct 2018; accepted 22 Oct 2018; published 26 Nov 2018

Optics EXPRESS

in IR lasers, like Ytterbium, Erbium and Thulium, the commercial microscope solutions cannot be used as they mostly features wavelength (VIS) and temporal resolutions (sub-µs) adapted to fluorophores important in biological or medical samples. They have to be adapted to excitations and emission wavelength of 1 to 2 µm and lifetimes of hundreds of µs to ms. Luckily, dopants in laser materials are non-moving.

It has been shown that confocal fluorescence microscopy has some other special advantages in the desired case. The probing volumes are small and waveguide effects as well as interaction effects typically distorting lifetime measurements like radiation trapping [10,11] can be minimized and allows to measure lifetime and PD effects accurately [12].

Due to the fact that novel developments especially in the topics of fiber laser tend towards advanced or novel material manufacturing methods, like reactive powder sintering of silica (REPUSIL) [13], sol-gel [14] or gas-phase doping [15], as well as more complex fiber structures [16], the measurements procedures along the production chain become more and more important. Thus, the specialized characterization methods beyond state-of-art need to be developed accordingly.

In this contribution, we investigate the application of a confocal fluorescence microscope setup to the measurement of optical parameters of Ytterbium (Yb) doped laser materials. In typical laser host materials, Yb shows a simple energy diagram, which is still sensitive to its host material [17]. After basic characterizations of the setup using well-known crystalline materials, we focus on Yb-doped fibers and preforms and analyze local optical parameters. Beside a fluorescence lifetime image (FLIM), micro-fluorescence emission spectroscopy (µSpec) imaging is done. Additionally, it is shown that PD can be measured spatially resolved as it influences the fluorescence lifetime and intensity. In an outlook, local saturation measurements are introduced to finally obtain parameters not yet accessible by other means. All parameters are highly important for manufacturing process evaluation and laser simulations of the doped material or fiber.

2. Measurement setup and evaluation procedures

Our setup shown in Fig. 1 is a scanning confocal fluorescence microscope [8,18] with excitation and fluorescence beam sharing the same path up to the dichroic mirror (high pass >940 nm). It is realized by modifying a Zeiss AxioScope Microscope. The excitation laser beam is emitted by a laser diode (LD) at 912 nm with up to 300mW to ensure highest excitation level. If not otherwise noted, 200 mW was the standard setting of the diode. This collimated beam enters the microscope via the illumination path for reflected light microscopy. Then the beam splitter (BS) or silver mirror (M), both set in the revolver turret, reflects the beam that gets focused by the microscope objective (MO, NA of 0.2) on an Ytterbium doped sample movable on an XY-stage. The MO also collects the emitted fluorescence. The fluorescence is taking the same way back but passing the dichroic mirror (DM) reflects the collimated beam with 99% to a single mode fiber providing the confocal pinhole and guiding the light to the optical spectrum analyzer (OSA, Yokogawa) for spectroscopic investigations or an avalanche photodiode (APD) for lifetime imaging.

Optics EXPRESS

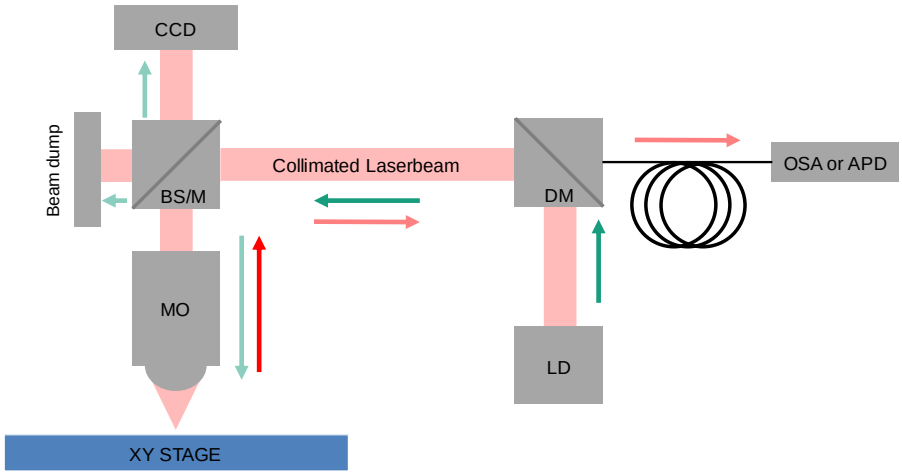

Fig. 1. Schematic representation of the setup: LD-laser diode, DM – dichroic mirror, BS – beam splitter, M – Mirror, MO – microscopic objective, OSA – optical spectrum analyzer, APD – avalanche photodiode. Green arrow: excitation direction, red arrow: Fluorescence signal direction.

First, the sample under test needs to be aligned. The beam splitter (BS) with the camera (CCD) is used for the rough alignment of the sample by imaging the Fresnel reflex of the excitation laser (with its wavelength close to the fluorescence signal to avoid chromatic aberrations) into that camera. All other light paths are aligned with it to give the optimum signal. Afterwards, we turn the revolver turret to a silver mirror (M). Afterwards, the measurement procedure is starting. The XY stage is positioned point by point while the OSA is detecting the spectral characteristics or the APD is measuring the temporal fluorescence decay when the laser diode switches off.

2.1 Resolution

In order to experimentally check the lateral resolution of the setup, we used a Yb:YAG sample, which is optically bonded to a non-doped YAG crystal at low temperatures [19] to secure that the Ytterbium's doping profile along the sample has a sharp edge in contrast to diffused profiles of, for instance, fiber preforms threated at high temperatures. The resolution cannot be resolved at an edge to the air, since the light propagates differently at this edge, which would give a resolution not comparable to the common doped material. A 4x15 μm^2 window was measured with 40 x 40 positions as shown in Fig. 2 and led to a resolution of 4 µm (10%-90% intensity criterion from Fig. 2(b)) matching the prediction for the NA of 0.2 of the used microscope objective.

For fiber/waveguide measurements, one has to keep in mind that wave-guiding effects may disturb the reliability of resolution. Although the measurement in the next sections seems to exclude this for the low guiding strength structures investigate, it is still important to keep in mind that light can be coupled into the guiding core.

Optics EXPRESS

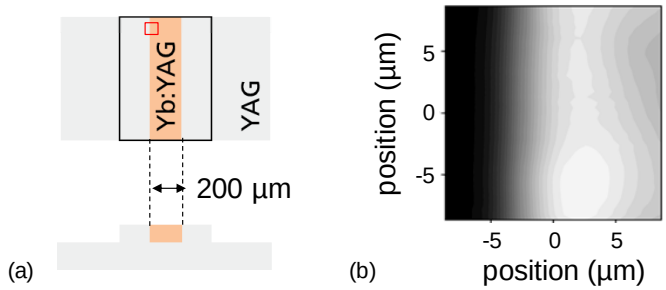

Fig. 2. (a) Schematic cross section and top view of the bonded Yb:YAG sample to a non-doped YAG and the measured region represented by the red rectangle, (b) section of the measured region representing the fluorescence intensity measurement on the edge of doped to undoped material (rotated 90° compared to (a)).

2.2 Lifetime and spectroscopic data processing

An oscilloscope catches the APD's response of fluorescence power after the laser has been shut down (shutdown in <10 µs). As the APD is noisy, the measurements are repeated several times to increase the signal-to-noise (SNR) ratio. Figure 3(a) shows an example trace and the stretched exponential fit for a non-average signal [20] according to

$$I(t) = I_0 \cdot e^{-(t/\tau)^{1/h}} \tag{1}$$

with the heterogeneity parameter h as a measure of the width of lifetime distribution. We have evaluated the heterogeneity h of all our samples and it can be concluded that a single exponential decay (h = 1) was enough in all cases to fit the lifetime, thus, the average lifetime and the fit parameter τ are equal and used in the following plots. In future work with special micro-structured fibers or preforms as well as production steps of Yb-doped materials, however, it could be possible that µm large areas of different doping environments with different lifetimes are investigated and will show a certain distribution of lifetimes and thus a parameter h different from 1.

For the spectroscopic analysis, a spectrum is recorded by the OSA from 900 nm to 1200 nm with a resolution of 2 nm as there are no fine features expected in doped glasses (see Fig. 2(b)). The wide spectral range allows to include the laser diodes Fresnel peak that leaks through the DM as well as the fluorescence of the sample to be recorded. In the following, we will show spectroscopic contrast that have been obtained by a simple fit of two Gaussian curves, one around 976 nm and around 1030nm central wavelength. An example of that fitting is shown in Fig. 3(b) for an Yb-doped fused silica glass preform. Of course, other parameters or a more precise fit can be obtained from the spectra if required. As will be shown, even the central wavelengths and FWHM of this simple fit will allow a good qualitative contrast as they are susceptible to chemical changes, for example the phosphorous co-doping.

In order to create a FLIM or µSpec image, the fluorescence intensity as the grey-scale image is multiplied with the information image – either the lifetime or any of the spectroscopic features giving the final image an additional color and information contrast.

Optics EXPRESS

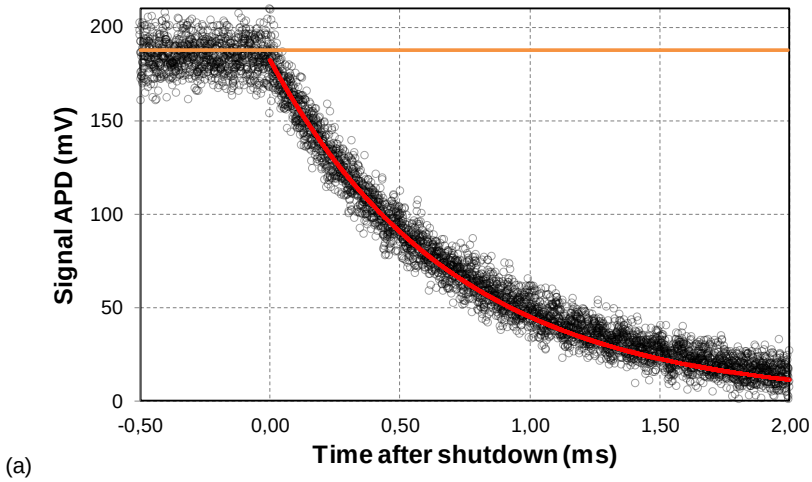

(a)

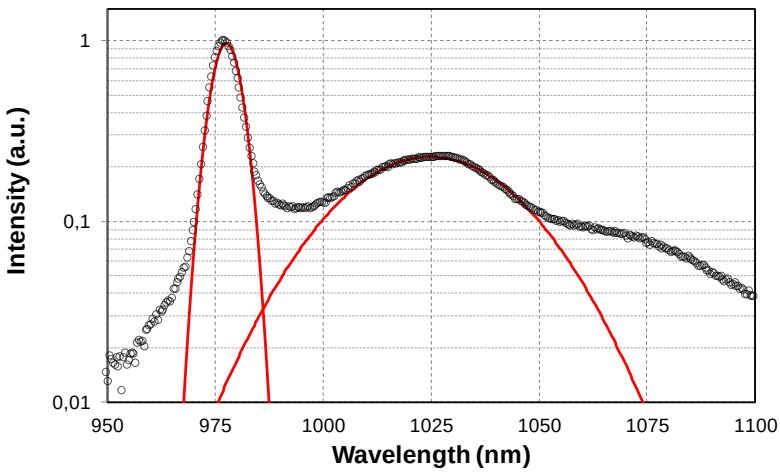

(b)

Fig. 3. (a) Oscilloscope trace of decaying ytterbium fluorescence and the fitted exponential decay (red) and intensity (orange), (b) Normalized spectrum of an Yb-doped fused silica sample with two Gaussian fits.

2.3 Validation of lifetime imaging

In order to confirm the validity of the lifetime measurements, we compared samples to literature values. Two samples were measured, a 1at% doped Yb:YAG sample and a 3at% doped Yb:CaF_2 sample. For those samples, lifetimes are reported in the literature [2,21]. Figure 4 illustrates the lifetimes as a histogram within the measurement area of samples, thus, each count is representing a measurement taken at a different spot of the sample. The individual measurement were repeated 16 times reducing the SNR. The lifetime distribution is either caused by the measurement error or by inhomogeneity in the samples composition. The reported lifetime values and variation (1σ) for Yb:YAG are 1.04 ms and for Yb:CaF_2 1.90 ± 0.10 ms. Our measured values of 1.03 ± 0.03 ms and 1.90 ± 0.03 ms are matching those.

Optics EXPRESS

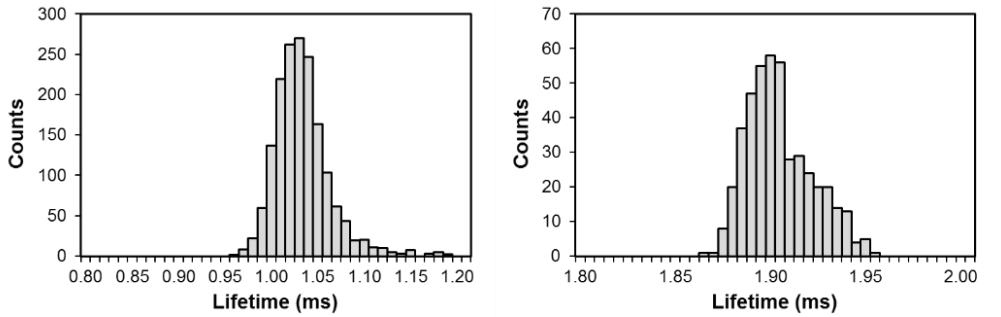

Fig. 4. Lifetime histogram of 1at% Yb:YAG (left) and 3at% Yb:CaF_2 (right).

We further judged our setup using nano-structured photonic crystal fibers. Due to their fabrication, the Yb-doped material is very homogeneous on a sub-micron scale, thus within the optical resolution. Additionally, those fibers exhibit interesting geometrical properties, which shall be able to be resolved. Figure 5 shows two examples as SEM images, which we measured with our setup. The first fiber is a reduced mode overlap (RMO) fiber shown in Fig. 5(a), which has been introduced to reduce PD and is pushed to kW output power [22,23]. The second fiber is also a double clad fiber with a special core geometry, which has an inner ring with large pitched air-holes, a so-called large-pitch fiber (LPF). Within this inner region, undoped and doped parts are introduced to provide preferential gain [16], which can be seen in Fig. 7(b) as a triangular shaped bright region.

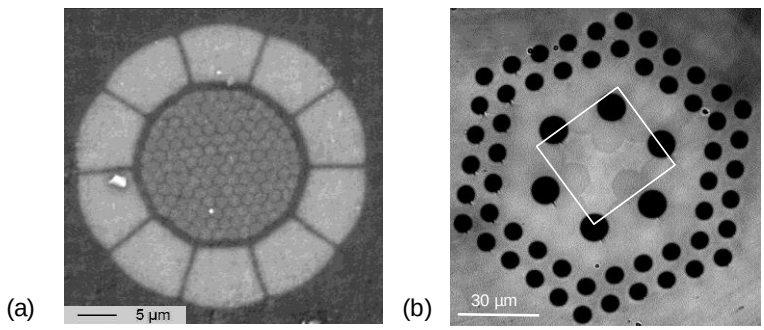

Fig. 5. SEM images of (a) RMO fiber and (b) LPF fiber with preferential gain region, which appears as a triangular brighter region (white box is the region of interest for Fig. 7).

In a first comparison, the fluorescence intensity image of our confocal setup is compared to a wide-field fluorescence intensity image, where the excitation has been done by side illumination. There, the excitation light sheet had a thickness of 60 µm and the MO again an NA of 0.2. This is two to three times thicker than the axial resolution of 25 µm of the confocal setup with the same MO. The results are shown in Fig. 6 depicting the nicely resolved Yb-doped out-of-core regions that are also visible in the SEM image in Fig. 5(a). The confocal image seems to have reduced out-of-focus light compared to the light sheet wide-field image.

Optics EXPRESS

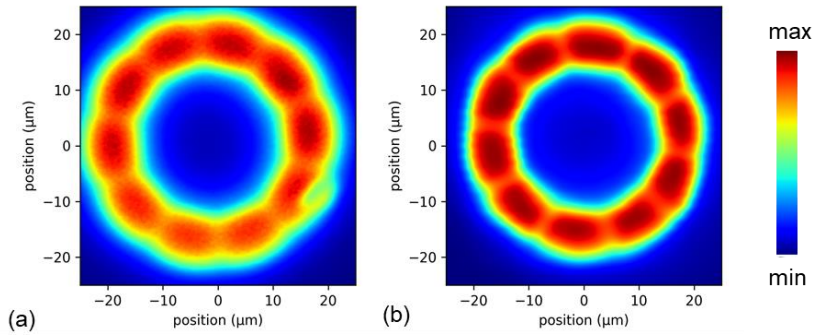

Fig. 6. Fluorescence intensity of the RMO fiber for (a) orthogonal excitation (light sheet) and (b) confocal measurement.

As such, nano-structured fibers feature an almost constant chemical environment on the scale of the resolution of the microscope, another test with these fibers is the lifetime distribution allowed by our measurement and fitting procedure. This is especially important as the lifetime data features most noise as can be seen in Fig. 3(a)). We use the LPF fiber from Fig. 5(b) and create a fluorescence lifetime image (FLIM image) as shown in Fig. 7. The color bar indicates the lifetimes and the weighted histogram is plotted aside. The lifetime does not correlate with intensity so the numerical fit is valid even at low intensities. The fluorescence lifetime was 860 +/– 26 µs. Similar values are obtained for the RMO fiber and especially the standard deviation of 26 µs lifetime can be seen as the "resolution" of lifetime in our setup and is the same as determined before. Similar to the lifetime, the µSpec images do not feature additional contrast, as the chemical environment is expected to be constant.

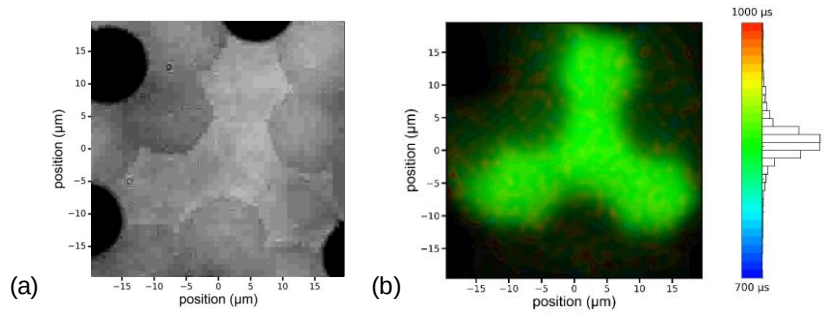

Fig. 7. (a) Zoom and rotated region of Fig. 5(b) and 5(b) the corresponding FLIM image of the LPF fiber with an average lifetime of 862 +/– 26 µs.

3. Examples of FLIM and µSpec images

3.1 Contrast and information enhancement

From bio-medical imaging, it is well-known that FLIM gives an additional information and contrast. In order to show this contrast for Yb-doped materials, we apply the method to Yb-doped material manufactured by REPUSIL [24]. This relatively new technique uses a silica powder as starting material. The desired dopants are added, so only doped silica material is created in this process. Due to silica particle arrangements as conglomerations, the created material may have features in the same size. Furthermore, inhomogeneity can occur on larger scales because of follow-up thermo-mechanical in the fabrication. It is therefore of importance to follow the process by characterization. We will show two examples during such processing steps highlighting FLIM and µSpec benefits, however, without going into the details of the physical explanation. This will be content of a separate publication.

Optics EXPRESS

Figure 8(a) is the FLIM measurement (125x120 measurement points) of the first, large sample to discuss, taken within the process steps toward REPUSIL material. A thermo-mechanical treatment in a strongly oxidizing environment was done to homogenies the material. The measurement reveals that the oxidizing environment creates an outer ring, which shows a lifetime as expected for that Yb-doped glass of ~850 µs. The lifetime in the inner area is 100µs shorter and the measured intensity about 30% decreased. Interestingly, this ring is not seen in an EPMA (electron micro probe analyzer) measurement and there are no changes in the fluorescence emission spectra as indicated by the µSpec image using the 1030 nm position and its spectral width as contrast in Fig. 8(b). Furthermore, an absorption measurement of the two regions showed a much higher absorption in the visible for the inner part compared to the outer ring as shown in Fig. 8(c).Without going into much detail, the oxidation of Yb^{2+} to Yb^{3+} due to the treatment would explain the difference. The remaining Yb^{2+} is reducing the intensity since it does not produce fluorescence around 1 µm and creates losses to the excited Yb^{3+} ions [10], as measured in Fig. 8(c). However, this loss cannot explain the intensity alone. It is furthermore known that Yb^{2+} reduces the fluorescence lifetime [25] and explains the strong contrast in the FLIM image. Further investigations shall reveal, which fabrication step is beneficial for homogenization and of course, its quality.

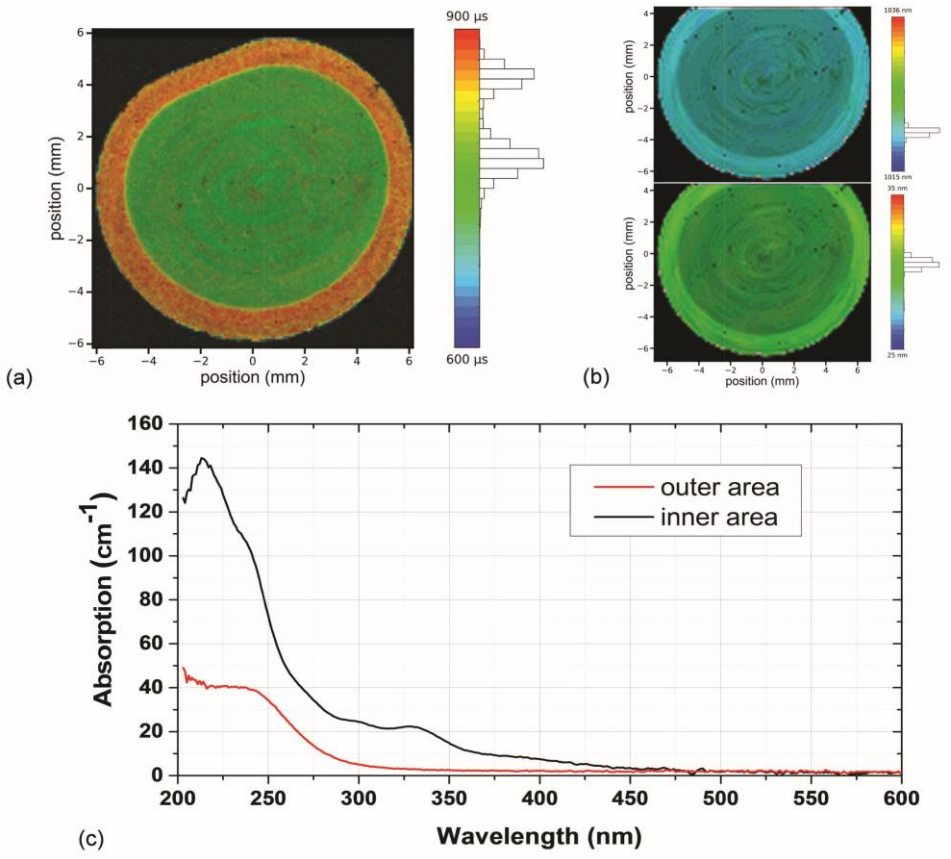

Fig. 8. (a) FLIM and (b) µSpec images with position (top) and width (bottom) of the emission peak around 1030 nm of a REPUSIL sample. (c) Corresponding absorption measurement at the inner and outer area.

The next sample of REPUSIL material is additionally thermo-mechanically treated. We used a thin, polished slice of 0.2 mm thickness for the FLIM image. Figure 9(a) shows the sample as seen by a microscope. The fluorescence intensity image shown in Fig. 9(b) does not

Optics EXPRESS

provide additional contrast. However, the FLIM image in Fig. 9(c) creates an additional lifetime contrast with strong lifetime variations compared to the lifetime intensity image or microscopic image alone.

From both samples, we conclude that the measurement technique will be very useful and enhances the analysis along the process chain.

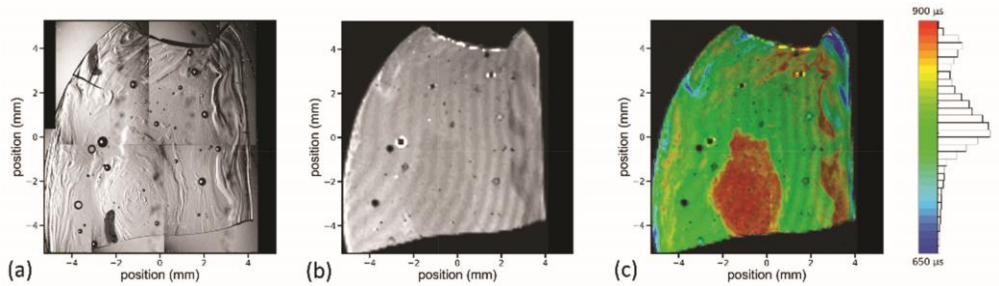

Fig. 9. Example for contrast and information enhancement: (a) Stitched microscopic image in comparison to (b) fluorescence intensity image and (c) FLIM image of the second REPUSIL sample.

3.2 Analysis of Yb-doped preforms and spatial resolved laser cross-section measurement

In this paragraph, special preforms are investigated using FLIM and µSpec resolving the spectral emission profile $I_{em}(\lambda,x,y)$ and the lifetime $\tau(x,y)$. The first sample is a preform made by modified chemical vapor deposition (MCVD) in combination with all-solution doping [26]. It consists of three different layers, which were intended to have different levels of Yb-doping and different ratios of Al:P in the layers [27]. Especially the inner layer was intended to not contain Phosphorous. Such complex structures are made to influence optical properties like mode area by flat top profile [28], improved single-mode low-NA fibers [29] and preferential ring-doping [30].

Because the local fluorescence depends on the chemical environment, these doping layers should be visible in the analysis. In order to have a reference on the doping profiles for Al, Yb and P, an EPMA measurement is done and shown in Fig. 10.

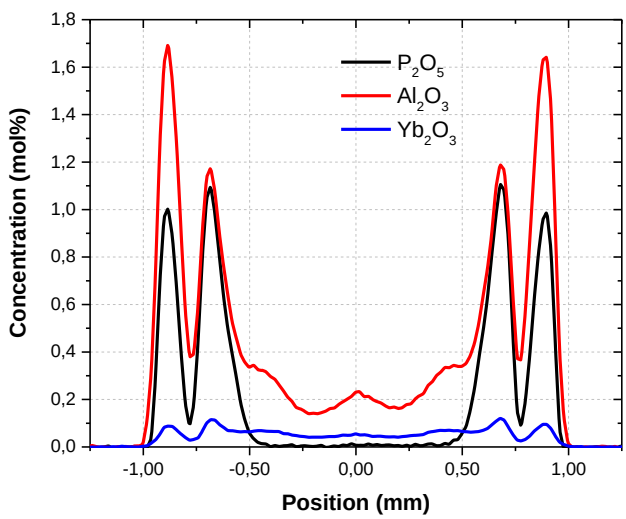

Fig. 10. EPMA measurement of the three-layered MCVD preform.

Optics EXPRESS

Figure 11 shows the result of the fluorescence imaging. In Fig. 11(a)-11(d), the measured emission spectrum is analyzed in terms of the peak position and FWHM of the 976 and 1030 nm fit as described before. For all these parameters, a significant contrast can be seen in the individual layers of the preform, which clearly indicate a change in the emission spectrum even at these low co-doping concentrations. In Fig. 11(e) the lifetime image is shown. The two outer layers contain Phosphorous and show a slightly higher lifetime compared to the inner layer. However, most contrast is seen in the µSpec images.

As the emission spectrum as well as the lifetime is spatially resolved, the emission cross section σ_{em} can be calculated by the Füchtbauer-Ladenburg-equation

$$\sigma_{em}(\lambda, x, y) = \frac{1}{8\pi \cdot n^2 \cdot c \cdot \tau_{rad}(\lambda, x, y)} \cdot \frac{\lambda^5 \cdot I_{em}(\lambda, x, y)}{\int \lambda \cdot I_{em}(\lambda, x, y)\, d\lambda} \tag{2}$$

where c is the velocity of light, n the material's refractive index, τ_{rad} the radiative lifetime of the upper state of the rare earth ion and I_{em} its spectral intensity. Figure 11(f) shows the emission cross sections for the three layers.

Optics EXPRESS

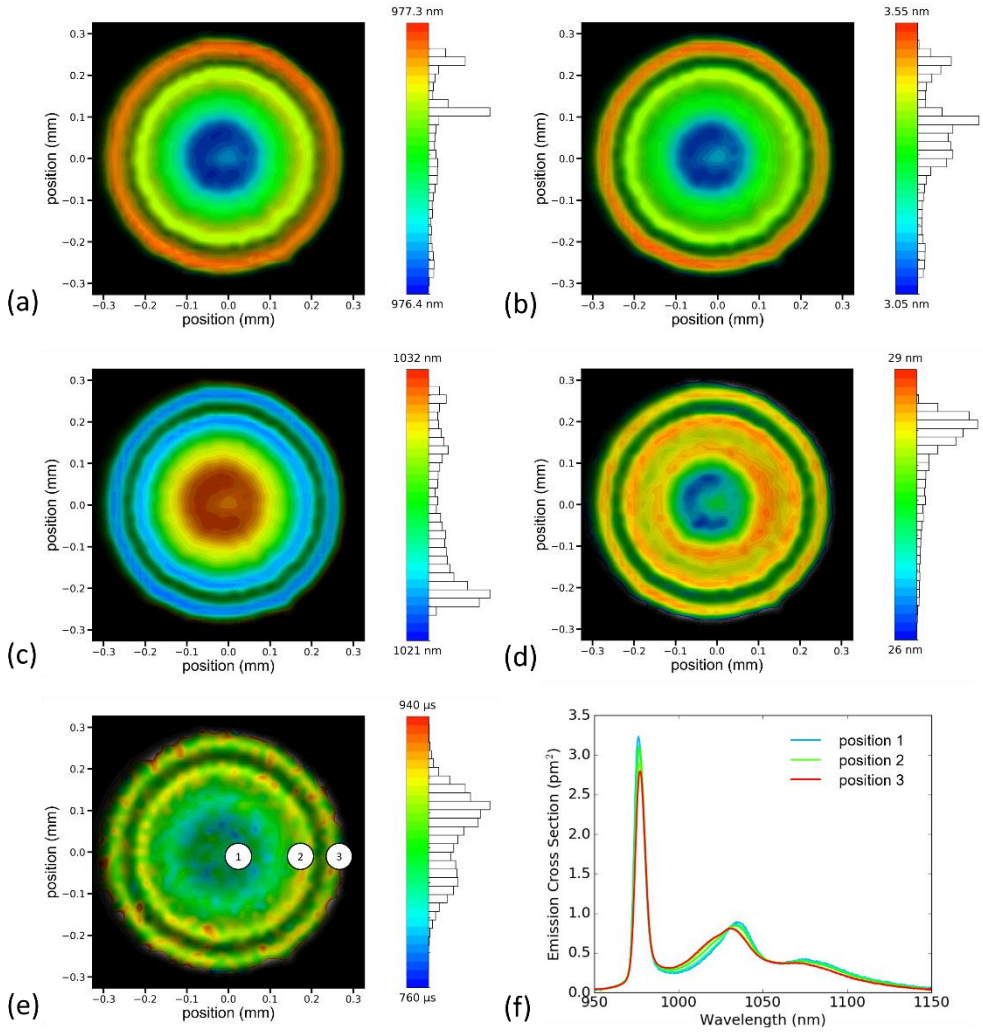

Fig. 11. µSpec image with (a) 976 nm central peak position, (b) 976 nm peaks FWHM, (a) 1030 nm central peak position, (b) 1030 nm peak FWHM as contrast and (e) FLIM with lifetime 857 +/– 30 µs (heterogeneity 1.03+/–0.03) and (f) emission cross section from center of preform (position 1) to outer region (position 3).

Finally, we compare the fluorescence intensity to the concentration profile measured by EPMA, Fig. 12(a). The concentration of the emitting ions c_{em} is related to the intensity and lifetime [31] by

$$c_{em} \sim I_{em} \cdot \tau \tag{3}$$

The data I_{em} is shown in Fig. 12(b). Also, the radial lifetime distribution is shown again to show that there is no strong variation of it, thus, the intensity itself is a good approximation for the concentration. A reasonable agreement is obtained in comparison to the EPMA measurements, despite the fact, that the errors in the EPMA measurement are also unknown. Additionally, it is shown that the FLIM and µSpec methods give very similar intensities, as expected. Nonetheless, without other methods we are not able to judge, which profile fits better to the actual concentration.

Optics EXPRESS

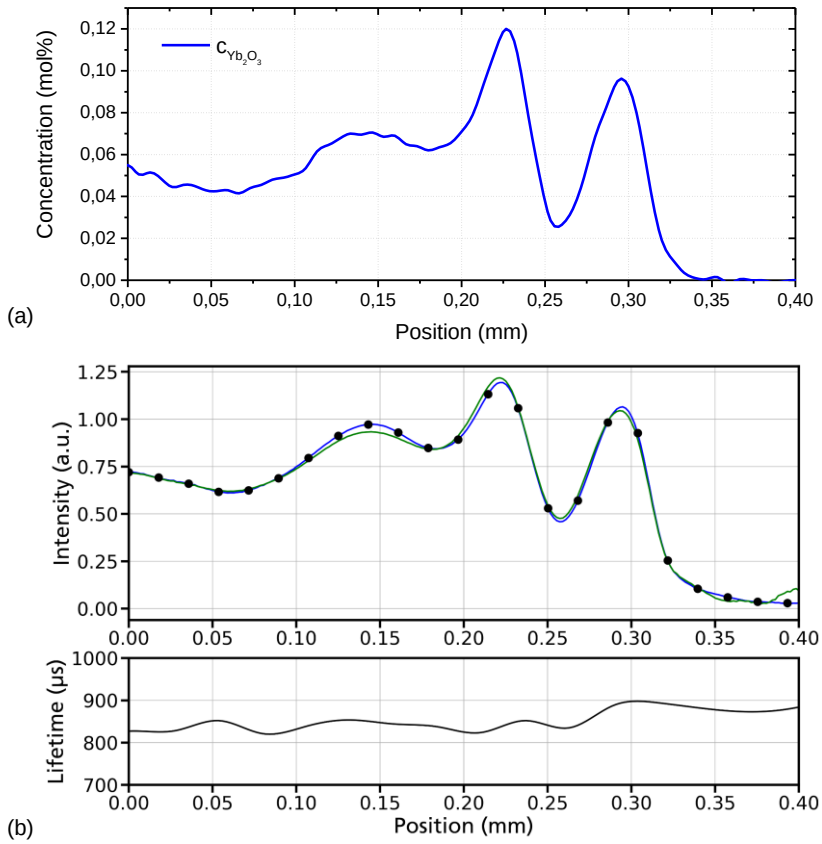

Fig. 12. (a) EPMA profile in comparison to (b, top) the shape of the radial averaged intensity as calculated from the FLIM intensity (blue and dots) and µSpec intensity data (green) and the radial lifetime distribution (b, bottom).

3.3 Photodarkening

The fluorescence signal is not only depended on the local chemical environment of the ion, it also is sensitive to quenching and PD issues of the material [32]. For the fiber preform samples so far, which had a doping level of 0.1mol%, PD has not been observed, since it increases with the square of the Ytterbium concentration and is proportional to the inversion level [6].

In Fig. 13 we used a highly Yb-doped fiber (1.5mol%) and started with a low inversion level by using only 20 mW of the excitation laser. The lifetime was measured to be 640 µs in the beginning and was already reduced after 60 s to 625 µs (Fig. 13(a)). In Fig. 13(b) the pump power was increased to 75 mW to increase the inversion. The lifetime started at 560 µs immediately and further decreased to below 550 µs in 60 s. This means that either care has to be taken if the material is susceptible to PD or, beneficially, one could measure the spatial resolved PD rate.

Optics EXPRESS

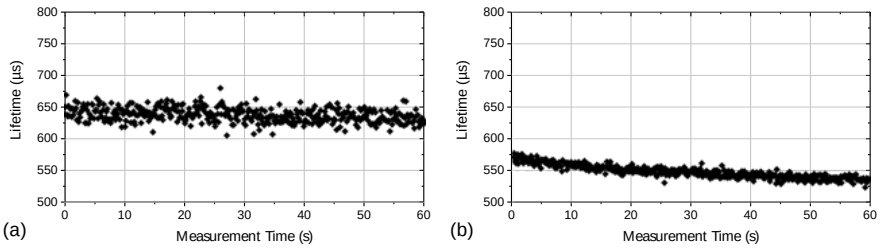

Fig. 13. (a) Decay of the measured lifetime with 20 mW pump power, (b) decay of lifetime with increased pump power of 75 mW for a measurement time of 60 seconds.

In order to demonstrate the possibility of a spatial resolved effect that PD initiated, we took a low-doped preform, which had been analyzed by EPMA with two perpendicular measurement traces across the center (cross). As the EPMA measurement uses an electron beam to generate an x-ray signal, the local material can be photo-darkened. Figure 14 shows the µSpec and FLIM images of the sample. In all images, the crossed analyzing traces of EPMA can be seen. The µSpec images mainly show a reduced intensity and the FLIM image reveals a lifetime reduction. Thus, this technique could be potentially used for fibers that reveals PD during laser operation to show potential transverse mode dependent effects [33], maybe in combination with higher resolutions by a high NA objective or super-resolution techniques [34] if required for the fiber's core dimensions.

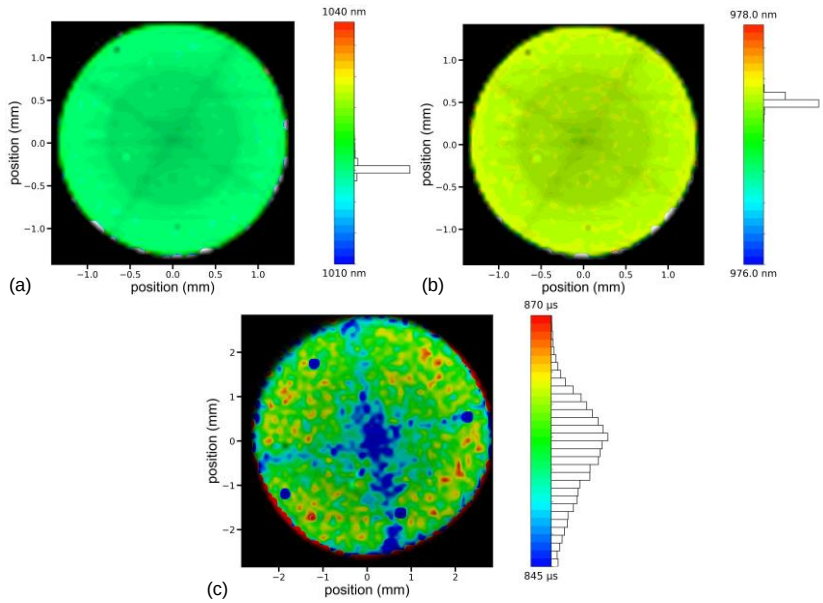

Fig. 14. Fluorescence analysis of a preform, which had been measured by EPMA before: (a) µSpec image for the 976 nm and (b) for the 1030 nm emission peak, (c) FLIM image.

4. Outlook

The setup and technique introduced so far can be enhanced further. For instance, by changing the pump power, the excitation level is change. It is well-known that the excitation level in the steady state will be saturated towards transparency according to

Optics EXPRESS

$$I_{em} = \mu \cdot \frac{1}{1 + \frac{\sigma_{em}}{\sigma_{abs}} + \frac{1}{\beta \cdot P_{pump}}} \tag{4}$$

where μ and β are independent scaling factors.

If this equation is fitted to the experimental data, the ratio of σ_{em} / σ_{abs} can be obtained directly and from this the maximum inversion $(1 + \sigma_{em} / \sigma_{abs})^{-1}$. An example is shown in Fig. 15, where the pump power has been slowly ramped up and the fluorescence signal is measured simultaneously. Unfortunately, the fit does not give reliable values yet and the variations are huge especially for the low-doped regions. To overcome this, the pump intensity needs to be varied over a huge dynamic range to ensure lowest and highest excitation for the fit curve to be clamped. This topic is currently under further investigation.

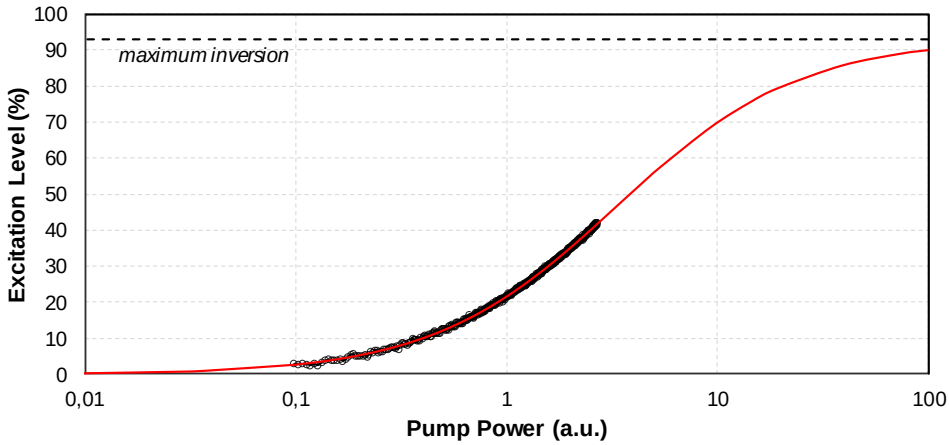

Fig. 15. Measured saturation of the fluorescence intensity level with respect to pump power and its fit to the excitation level.

5. Conclusion

It could be shown that the presented confocal fluorescence microscope system adapted to Yb-doped materials is very useful for determination of fluorescent ion concentration, upper-state lifetime distribution and emission cross sections in a spatially resolved way. Examples are given for crystals, fibers and preforms to show that even small changes in the chemical environment can be detected and a useful contrast is obtained from lifetime and spectral data. Furthermore, qualitative imaging of REPUSIL and MCVD specimens show the importance of observing the preform fabrication process. Other aspects of PD have been discussed and seem to be promising in the future application of this technique.

Funding

BMBF (13N13652); State of Thuringia supported by EU programs EFRE and ESF (2015FOR0017, 13030-715, 2011FGR0104, 2015FGR0107, 2015FGR0108, B715-11011, B715-11005).

References

1. M. N. Zervas and C. A. Codemard, “High Power Fiber Lasers. A Review,” IEEE J. Sel. Top. Quantum Electron. **20**(5), 219–241 (2014).
2. K. Petermann, D. Fagundes-Peters, J. Johannsen, M. Mond, V. Peters, J. J. Romero, S. Kutovoi, J. Speiser, and A. Giesen, “Highly Yb-doped oxides for thin-disc lasers,” J. Cryst. Growth **275**(1-2), 135–140 (2005).
3. F. Beier, F. Möller, B. Sattler, J. Nold, A. Liem, C. Hupel, S. Kuhn, S. Hein, N. Haarlammert, T. Schreiber, R. Eberhardt, and A. Tünnermann, “Experimental investigations on the TMI thresholds of low-NA Yb-doped single-mode fibers,” Opt. Lett. **43**(6), 1291–1294 (2018).

Optics EXPRESS

4. H.-J. Otto, N. Modsching, C. Jauregui, J. Limpert, and A. Tünnermann, "Impact of photodarkening on the mode instability threshold," Opt. Express **23**(12), 15265–15277 (2015).
5. F. Sidiroglou, A. Roberts, and G. Baxter, "Contributed Review: A review of the investigation of rare-earth dopant profiles in optical fibers," Rev. Sci. Instrum. **87**(4), 041501 (2016).
6. A. Schwuchow, S. Unger, S. Jetschke, and J. Kirchhof, "Advanced attenuation and fluorescence measurement methods in the investigation of photodarkening and related properties of ytterbium-doped fibers," Appl. Opt. **53**(7), 1466–1473 (2014).
7. A. D. Yablon, "New transverse techniques for characterizing high-power optical fibers," Opt. Eng. **50**(11), 111603 (2011).
8. S. Inoué, "Foundations of Confocal Scanned Imaging in Light Microscopy," in *Handbook of Biological Confocal Microscopy*, J. B. Pawley, ed. (Springer US, 1995), pp. 1–14.
9. K. Suhling, L. M. Hirvonen, J. A. Levitt, P.-H. Chung, C. Tregidgo, D. A. Rusakov, K. Zheng, S. Ameer-Beg, S. Poland, S. Coelho, R. Henderson, and N. Krstajic, "Fluorescence Lifetime Imaging," in *Handbook of Photonics for Biomedical Engineering*, A. H.-P. Ho, D. Kim, and M. G. Somekh, eds. (Springer Netherlands, 2014), pp. 1–50.
10. D. S. Sumida and T. Y. Fan, "Effect of radiation trapping on fluorescence lifetime and emission cross section measurements in solid-state laser media," Opt. Lett. **19**(17), 1343–1345 (1994).
11. H. Kühn, S. T. Fredrich-Thornton, C. Kränkel, R. Peters, and K. Petermann, "Model for the calculation of radiation trapping and description of the pinhole method," Opt. Lett. **32**(13), 1908–1910 (2007).
12. Y.-S. Yong, S. Aravazhi, S. A. Vázquez-Córdova, J. J. Carvajal, F. Díaz, J. L. Herek, S. M. García-Blanco, and M. Pollnau, "Direct confocal lifetime measurements on rare-earth-doped media exhibiting radiation trapping," Opt. Mater. Express **7**(2), 527 (2017).
13. A. Langner, G. Schötz, M. Such, T. Kayser, V. Reichel, S. Grimm, J. Kirchhof, V. Krause, and G. Rehmann, "A new material for high-power laser fibers," Proc. SPIE **6873**, 687311 (2008).
14. D. Etissa, M. Neff, S. Pilz, M. Ryser, and V. Romano, "Rare earth doped optical fiber fabrication by standard and sol-gel derived granulated oxides," Proc. SPIE **8426**, 84261I (2012).
15. S. Unger, F. Lindner, C. Aichele, M. Leich, A. Schwuchow, J. Kobelke, J. Dellith, K. Schuster, and H. Bartelt, "A highly efficient Yb-doped silica laser fiber prepared by gas phase doping technology," Laser Phys. **24**(3), 035103 (2014).
16. T. Eidam, S. Hädrich, F. Jansen, F. Stutzki, J. Rothhardt, H. Carstens, C. Jauregui, J. Limpert, and A. Tünnermann, "Preferential gain photonic-crystal fiber for mode stabilization at high average powers," Opt. Express **19**(9), 8656–8661 (2011).
17. M. Weber, J. Lynch, D. Blackburn, and D. Cronin, "Dependence of the stimulated emission cross section of Yb^{3+} on host glass composition," IEEE J. Quantum Electron. **19**(10), 1600–1608 (1983).
18. K. P. Ghiggino, M. R. Harris, and P. G. Spizzirri, "Fluorescence lifetime measurements using a novel fiber-optic laser scanning confocal microscope," Rev. Sci. Instrum. **63**(5), 2999–3002 (1992).
19. C. Rothhardt, S. Risse, T. Schreiber, R. Eberhardt, J. Rothhardt, J. Limpert, and A. Tünnermann, "Direct Bonding of Crystalline Components for Application in High Power Laser Systems," in *Laser Ignition Conference. 20–23 June 2017, Bucharest, Romania*, OSA technical digest (online) (OSA - The Optical Society, 2017), LWA3.4.
20. K. C. Lee, J. Siegel, S. E. D. Webb, S. Lévêque-Fort, M. J. Cole, R. Jones, K. Dowling, M. J. Lever, and P. M. W. French, "Application of the stretched exponential function to fluorescence lifetime imaging," Biophys. J. **81**(3), 1265–1274 (2001).
21. J. Koerner, C. Vorholt, H. Liebetrau, M. Kahle, D. Kloepfel, R. Seifert, J. Hein, and M. C. Kaluza, "Measurement of temperature-dependent absorption and emission spectra of Yb:YAG, Yb:LuAG, and Yb:CaF_2 between 20 °C and 200 °C and predictions on their influence on laser performance," J. Opt. Soc. Am. B **29**(9), 2493–2502 (2012).
22. K. E. Mattsson, "Low photo darkening single mode RMO fiber," Opt. Express **17**(20), 17855–17861 (2009).
23. N. Haarlammert, B. Sattler, A. Liem, M. Strecker, J. Nold, T. Schreiber, R. Eberhardt, A. Tünnermann, K. Ludewigt, and M. Jung, "Optimizing mode instability in low-NA fibers by passive strategies," Opt. Lett. **40**(10), 2317–2320 (2015).
24. K. Schuster, S. Unger, C. Aichele, F. Lindner, S. Grimm, D. Litzkendorf, J. Kobelke, J. Bierlich, K. Wondraczek, and H. Bartelt, "Material and technology trends in fiber optics," Adv. Opt. Technol. **3**(4), 447–468 (2014).
25. J. Kirchhof, S. Unger, A. Schwuchow, S. Grimm, and V. Reichel, "Materials for high-power fiber lasers," J. Non-Cryst. Solids **352**(23-25), 2399–2403 (2006).
26. S. Kuhn, S. Hein, C. Hupel, J. Ihring, J. Nold, N. Haarlammert, T. Schreiber, R. Eberhardt, and A. Tünnermann, "All-Solution Doping Technique for Tailoring Core Composition toward Yb:$AlPO_4$:SiO_2," in Advanced Solid State Lasers, OSA Technical Digest (online) (Optical Society of America, 2015), paper AM4A.5.
27. S. Kuhn, S. Hein, C. Hupel, J. Nold, N. Haarlammert, T. Schreiber, R. Eberhardt, and A. Tünnermann, "Modelling the refractive index behavior of Al,P-doped SiO_2, fabricated by means of all-solution doping, in the vicinity of Al:P = 1:1," Opt. Mater. Express **8**(5), 1328–1340 (2018).
28. A. K. Ghatak, I. C. Goyal, and R. Jindal, "Design of a waveguide refractive index profile to obtain a flat modal field," Proc. SPIE **3666**, 40–44 (1999).

Optics EXPRESS

29. D. Jain, Y. Jung, M. Nunez-Velazquez, and J. K. Sahu, "Extending single mode performance of all-solid large-mode-area single trench fiber," Opt. Express **22**(25), 31078–31091 (2014).
30. J. Nilsson, R. Paschotta, J. E. Caplen, and D. C. Hanna, "Yb^3+)-ring-doped fiber for high-energy pulse amplification," Opt. Lett. **22**(14), 1092–1094 (1997).
31. I. R. Perry, A. C. Tropper, and J. R. M. Barr, "Micro-fluorescence profiling of erbium-doped fibre preforms," J. Lumin. **59**(1–2), 39–49 (1994).
32. R. Paschotta, J. Nilsson, P. R. Barber, J. E. Caplen, A. C. Tropper, and D. C. Hanna, "Lifetime quenching in Yb-doped fibres," Opt. Commun. **136**(5-6), 375–378 (1997).
33. C. Jauregui, T. Eidam, H.-J. Otto, F. Stutzki, F. Jansen, J. Limpert, and A. Tünnermann, "Physical origin of mode instabilities in high-power fiber laser systems," Opt. Express **20**(12), 12912–12925 (2012).
34. E. Auksorius, B. R. Boruah, C. Dunsby, P. M. P. Lanigan, G. Kennedy, M. A. A. Neil, and P. M. W. French, "Stimulated emission depletion microscopy with a supercontinuum source and fluorescence lifetime imaging," Opt. Lett. **33**(2), 113–115 (2008).